

A Novel Synthetic Compound, Bismuth Zinc Citrate, Could Potentially Reduce Cisplatin-Induced Toxicity Without Compromising the Anticancer Effect Through Enhanced Expression of Antioxidant Protein



Shing Chan^{*,1}, Runming Wang^{†,1}, Kwan Man[‡], John Nicholls[§], Hongyan Li[†], Hongzhe Sun[†] and Godfrey Chi-Fung Chan^{*}

^{*}Department of Paediatrics & Adolescent Medicine, LKS Faculty of Medicine, The University of Hong Kong; [†]Department of Chemistry, Faculty of Science, The University of Hong Kong; [‡]Department of Surgery, LKS Faculty of Medicine, The University of Hong Kong; [§]Department of Pathology, LKS Faculty of Medicine, The University of Hong Kong

Abstract

Cisplatin is a common anticancer drug, but it comes with significant nephrotoxicity. Further cisplatin-induced oxidative stress contributes to the pathogenesis of the nephrotoxicity. A new compound, BiZn, can potentially prevent this complication. We verified our postulation by *in vitro* and *in vivo* models. From our findings, BiZn did not affect cisplatin-induced cytotoxicity on neuroblastoma cells under both *in vitro* and *in vivo* settings. However, BiZn significantly reduced the blood urea nitrogen and creatinine levels in cisplatin-treated mice. Under the lethal dosage of cisplatin, co-treatment of BiZn significantly increased the survival rate. BiZn stimulated antioxidant proteins metallothionein (MT) and glutathione (GSH) generation from kidney cells and minimized cisplatin-induced apoptosis. Knocking down MT-IIA and inhibiting GSH abolished such protection. In conclusion, pretreatment of BiZn decreased cisplatin-induced renal toxicity without affecting its antitumor activity. BiZn-induced antioxidant proteins MT and GSH may contribute to the renal protection effect.

Translational Oncology (2019) 12, 788–799

Introduction

Cisplatin is a commonly used anticancer drug for solid tumors. However, it suffers significant side effects including nephrotoxicity, ototoxicity, and myelotoxicity, thus hindering its wide clinical application in selected patients [1–5]. Around 25% to 35% of patients who received cisplatin treatments experienced various degrees of nephrotoxicity [6]. It is well known that reactive oxygen species (ROS) are greatly involved in the pathogenesis of nephrotoxicity [7]. Current protective agents such as amifostine have significant side effects including hypotension, hypocalcemia, nausea, vomiting, allergies, and skin toxicities and may affect the anticancer efficacy of cisplatin, so it has not been widely adopted as standard treatment [8,9]. Therefore, we developed a novel bismuth compound, BiZn, to investigate whether it can protect renal cells against cisplatin-induced damage.

MT and glutathione (GSH) are the two key thiols that prevent cellular injury from either heavy metals or oxidative damage in mammalian cells [10,11]. MT is a low-molecular weight cysteine-

rich intracellular protein, which plays an important role in the detoxification of toxic heavy metals [12–14]. Moreover, it has been demonstrated that MT has an antioxidant property by scavenging for free radicals [15,16]. GSH plays an important role in the regulation of cell cycle, including proliferation and death. GSH is a known antioxidant involved in protecting cells from the noxious effect of

Address all correspondence to: Sun Hongzhe, Department of Chemistry, Faculty of Science, The University of Hong Kong, or Chan Godfrey Chi-Fung, Department of Paediatrics & Adolescent Medicine, LKS Faculty of Medicine, The University of Hong Kong.

E-mails: hsun@hku.hk, hsun@hku.hk

¹Chan Shing & Wang Runming are both first authors.

Received 7 August 2018; Revised 14 February 2019; Accepted 14 February 2019

© 2019 Published by Elsevier Inc. on behalf of Neoplasia Press, Inc. This is an open access article under the CC BY-NC-ND license (<http://creativecommons.org/licenses/by-nc-nd/4.0/>).

1936-5233/19

<https://doi.org/10.1016/j.tranon.2019.02.003>

excessive oxidant stress [17]. It has been shown to reduce toxicity and improve the quality of life of cisplatin-treated cancer patients [18]. Therefore, any new drugs that can induce the local generation of MT and GSH in order to provide localized organ protection in cancer patients receiving cisplatin therapy will be benefit for cancer patients. Bismuth is relatively nontoxic metal ion and has long been associated with medicine [19], and our group has concentrated on this field of study for many years [20–24]. Zinc (Zn^{2+}) and bismuth (Bi^{3+}) are found to induce the synthesis of a special protein MT in the kidney [25,26]. Whether our new compound induces the synthesis of both MT and GSH is still unknown. Most importantly, whether the new compound could alleviate cisplatin-induced nephrotoxicity *in vitro* and *in vivo* is subject to further evaluation.

In this study, we prepared the bismuth compound, BiZn, to investigate its potential protective effects on different nonmalignant human cell types including kidney cells (HK-2), mesenchymal stromal cells (mesenchymal stem cells or MSC), liver cells (MIHA), and rat neural stem cells (C17.2) as well as a neuroblastoma cell line (SKNLP) *in vitro*. Whether BiZn could induce generation of antioxidant proteins MT and GSH from HK-2 cells and the possible protective effect of BiZn on cisplatin-induced renal toxicity *in vivo* were also studied. Finally, the long-term effect of BiZn on the antitumor activity of cisplatin treated mice was investigated using orthotopic xenograft model for 3 weeks.

Materials and Methods

Chemicals

Cisplatin was purchased from Mayne Pharma Pty Ltd., Mulgrave, VIC 3170, Australia. BiZn ($BiCit_2Zn$, MW 689.13) was prepared with the following procedures. Briefly, bismuth citrate (2 mmol, 0.80 g) was dissolved in deionized water (20 ml), while 18% ammonia was gradually added until the suspension became clean. Appropriate amount of $Zn(OH)_2$ was added slowly over a time course of 24 hours to the bismuth-ammonia aqueous solution to result in a fully saturated solution. Any impurity was filtered off. The solution was left for 1 week for the production of crystal-like product. BiZn: ESI-MS m/z + ve: 689.13 ($[Bi(cit)_2Zn]^+$, 100%), 727.07 ($[Bi(cit)_2Zn + K]^+$, 85%) The chemical structure was shown in Figure 1. L-buthionine-sulfoximine (BSO) was purchased from Sigma-Aldrich Co.

Cell Lines

Human bone marrow-derived mesenchymal stromal cells (MSC), human nonmalignant liver cells (MIHA), rat neural stem cells (C17.2) and human nonmalignant kidney cells (HK-2, provided by Dr. Yang Mo, Department of Pediatrics, Nanfang Hospital, Southern Medical University, Guangdong, China) and tumor SKNLP (provided by Dr. Nai Kong Cheung, Memorial Sloan Kettering Cancer Center, New York, NY) were cultured in DMEM (GIBCO Laboratories, Renfrewshire, UK) supplemented with 10% fetal calf serum (GIBCO Laboratories, Renfrewshire, UK).

Cell Proliferation Assay

The growth and viability characteristics from the effect of BiZn on cisplatin-treated MSC, MIHA, C17.2, and HK-2 cells as well as SKNLP cells were measured using the cell proliferation kit II XTT assay (Roche Diagnostics, USA, according to the manufacturer's instruction). A total of $1-2 \times 10^4$ cells/well were grown in flat-bottom 96-well plates (Costar, Corning Incorporated, NY) in a final volume

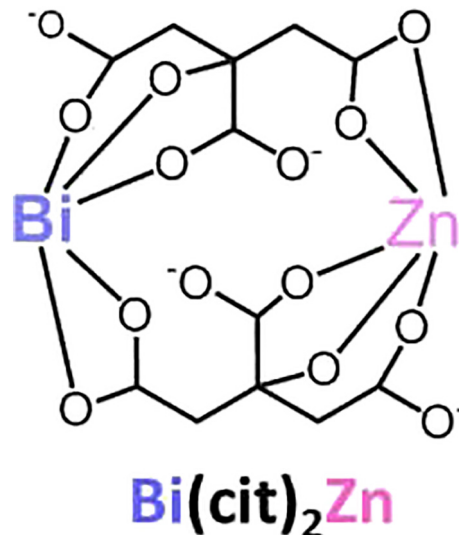


Figure 1. Chemical structure of bismuth zinc citrate.

of 100 μ l culture medium per well overnight. Cells were then exposed to BiZn (10 μ M or 100 μ M) for 2 hours before treatment with cisplatin (10 μ M or 100 μ M) for 2 or 3 days. For GSH study in Figure 5, HK-2 cells were exposed to BiZn (10 μ M or 100 μ M) for 6 hours, and after 3 days, they were treated with cisplatin (10 μ M) and BSO (500 μ M) for 2 more days. Cells grown under culture medium alone were used as a negative control. After a fixed time of incubation, 50 μ l of the XTT labeling mixture was added to each well, and the cells were incubated for 2 hours at 37°C under a humidified atmosphere of 5% CO_2 . The formation of formazan dyes, produced only by metabolic active cells, was detected spectrophotometrically at 490 nm.

Neutral Red Uptake Assay

A neutral red uptake assay was performed following the procedure as described by Borenfreund and Puerner et al. [27]. Briefly, $1-2 \times 10^4$ cells/well were seeded in 96-well plates and then exposed to BiZn (10 μ M or 100 μ M) for 6 hours, and after 3 days, they were treated with cisplatin (10 μ M) and BSO (500 μ M) for 2 more days. At the end of the exposure time, the test solution was aspirated and cells were washed with phosphate-buffered saline (PBS) twice before being incubated for 2 hours in medium supplemented with neutral red (50 μ g/ml). The medium was washed off rapidly with a solution containing 0.5% formaldehyde and 1% calcium chloride. The cells were then incubated for a further 20 minutes at 37°C in a mixture of acetic acid (1%) and ethanol (50%) to extract the dye. The absorbance was detected spectrophotometrically at 540 nm.

Measurement of Oxidative Stress

Intracellular production of ROS in HK-2 cells treated with cisplatin and BiZn was monitored using a 2',7'-dichlorodihydrofluorescein diacetate (H_2DCFDA) fluorescent probe (Sigma). H_2DCFDA is deacetylated by intracellular esterases to form 2',7'-dichlorodihydrofluorescein. In the presence of hydrogen peroxides and hydroxyl radicals in cells, it will be converted to the fluorescent 2',7'-dichlorofluorescein (DCF). To quantify ROS production, HK-2 cells were resuspended in DMEM with 10% FBS. BiZn was added to the cells for a 24-hour pretreatment. Cisplatin was then added to the HK-2 cells and incubated for 4 hours before H_2DCFDA staining. Cells were treated with H_2DCFDA (5 μ M) in PBS at 37°C. The

DCF fluorescence produced by the cells was measured continuously on a fluorometer at an excitation wavelength of 485 nm and emission wavelength of 538 nm.

Western Blotting

HK-2 and MIHA cells were treated with BiZn (100 μ M) for 0 to 24 hours. Cells were washed with ice-cold PBS, and cell lysates were extracted by protein extraction solution. Protein concentration was determined by the Quick Start Bradford 1 \times Dye Reagent (Bio-Rad Laboratories, Inc., USA). Proteins were loaded on SDS-PAGE gels and separated by electrophoresis. The gels were transferred to nitrocellulose membrane and blocked within 5% BSA in Tris-buffered saline solution containing 0.1% Tween-20. Primary antibodies, mouse anti-MT monoclonal antibody (1:1000 dilution; Abcam, USA), were incubated overnight at 4°C. After washing, the membrane was incubated with a secondary antibody, rabbit anti-mouse antibody (1:2000 dilution; Cell Signaling Technology, Beverly, MA, USA). MT was visualized by ECL detection systems.

RNA Isolation

Total RNA was prepared according to the protocol using Trizol (Invitrogen) solution. Trizol (500 μ l) was added to HK-2 cells which were treated with BiZn for 6 hours. Chloroform (100 μ l) was then added to the sample. The suspension was centrifuged at 12000 \times g for 15 minutes at 4°C. After the phase separation, the upper aqueous phase was then transferred to a new tube, and RNA precipitation was done by adding 500 μ l of isopropanol. After thorough mixing and storage at room temperature for 15 minutes, the suspension was centrifuged at 12,000 \times g for 15 minutes at 4°C. After the isopropanol was decanted, the remaining RNA pellet was then washed with 75% ethanol and centrifuged at 12,000 \times g. The pellet was then air-dried and resuspended in DEPC water. The concentration and purity of each sample were evaluated using a spectrophotometer at A260/A280.

Quantitative Reverse-Transcription Polymerase Chain Reaction

Expression of mRNA was analyzed in HK-2 cells using qRT-PCR. One microgram of HK-2 cell RNA was reverse transcribed using reverse transcriptase II (Invitrogen) according to the manufacturer's instructions. Real-time qPCR was performed using PowerUp SYBR Green Master Mix (Thermo Fisher Scientific) in ABI PRISM 7900 real-time PCR system (Applied Biosystems). The real-time qPCR was in the presence of 1 \times PowerUp SYBR Green Master Mix and 0.2 μ M of each gene Q-PCR primer. Two primer pair sequences were synthesized for human MT-IA and MT-IIA genes as described by Liu et al. [24] to amplify a fragment encompassing the coding region of the MT gene. The amplification profile was 50°C for 2 minutes and 95°C for 2 minutes followed by 40 cycles of 95°C for 15 seconds and 60°C for 1 minute. At the end of the PCR cycles, melting curve analyses were performed to ensure the absence of artifacts. Three biological replicates were measured for each group. The expression levels of mRNAs were normalized to glyceraldehyde 3-phosphate dehydrogenase (GAPDH) level 5'-ACCACAGTCCATGCCATCACT for the sense and 5'-GGCCATCACGCCACAGTT for the antisense. The fold change of the mRNA was calculated by the equation $2^{-\Delta\Delta C_t}$.

Establishment of shRNA Knockdown Cell Lines

MT-IIA shRNA Plasmids (Santa Cruz Biotechnology, CA, USA), encoded with three short hairpin RNAs (shRNAs), was transfected

into HK-2 cell lines to establish the knockdown cell line models. The scrambled shRNA Plasmid-A (Santa Cruz Biotechnology, CA, USA) served as a mock transfection vector. Transfection was performed according to manufacturer's instructions with modifications. Cells were first seeded in a 24-well plate and grown to 70% confluence. One day prior to transfection, normal culture medium was removed and replaced with 500 μ l antibiotic-free DMEM (supplemented with 10% FBS). For each transfection, 1 μ g of MT-IIA shRNA plasmid was resuspended in 50 μ l FBS-free OptiMEM; 3 μ l Lipofectamine 2000 (Invitrogen, CA, USA) was diluted in 50 μ l serum-free OptiMEM and incubated for 5 minutes at room temperature. The two solutions were gently mixed and allowed to sit for 20 minutes at room temperature. One hundred microliters of this combined solution was added to each well containing cells and medium with gentle mixing. Cells were then incubated at 37°C with 5% carbon dioxide for 6 hours. After the incubation, DMEM with 2 mM l-glutamine, 10% FBS, and 2 μ g/ml puromycin (Invitrogen GIBCO, NY, USA) was added as a selective medium to establish the stable MT-IIA knockdown cell lines.

Measurement of Intracellular Reduced GSH Using Monochlorobimane Assay and GSH Detection Assay

Reduced GSH in HK-2 cells treated with BiZn (10 μ M and 100 μ M) for 24 and 48 hours was monitored using monochlorobimane assay (Sigma, USA). This probe reacts specifically with reduced GSH through GSH transferase to form a fluorescent derivative [28]. To investigate the GSH production, HK-2 cells were resuspended in DMEM with 10% FCS. BiZn (10 μ M or 100 μ M) and L-buthionine-sulfoximine (BSO) (250 μ M or 500 μ M) (Sigma, USA) were added to the cells respectively for 24 or 48 hours. The cells were treated with monochlorobimane (Sigma, USA) at a final concentration of 100 mM in Ca²⁺- and Mg²⁺-free PBS for 0 to 60 minutes at 37°C. The fluorescence produced by the cells was measured with a fluorometer at an excitation wavelength of 360 nm and emission wavelength of 480 nm.

Reduced GSH in samples was measured by using GSH Detection Assay Kit (Abcam). Briefly, HK-2 cells were treated with BiZn (10 μ M and 100 μ M) for 48 hours. A total of 0.2×10^6 cells were homogenized by Mammalian Lysis Buffer. Enzymes were removed by using Deproteinizing Sample Kit (Abcam). Nonfluorescent GSH Assay Mixture reacts with reduced GSH in cell lysate to become fluorescent. The fluorescence produced was measured with a fluorometer at an excitation wavelength of 490 nm and emission wavelength of 520 nm.

Animals and Drug Treatment

All experiments were performed on 5- to 6-week-old male mice (Laboratory Animal Unit, the University of Hong Kong). The mice were housed under specific pathogen free conditions and were given free access to water and food. All animal experiments were done in accordance with the University of Hong Kong Guideline for Animal Care and Experimentation. After transfection of SKNLP neuroblastoma cell line with a luciferase construct, we injected the stable luciferase positive cells into the adrenal glands (2×10^5 cells) of SCID Beige mice. Orthotopic neuroblastoma cancer xenograft models were established within 1 month. We divided the mice into four groups: control ($n = 6$), BiZn-treated ($n = 6$), cisplatin-treated ($n = 6$), and BiZn plus cisplatin-treated ($n = 6$) groups. The BiZn (0.14 mmol/kg) was administered orally. Cisplatin (7.5 mg/kg or 15 mg/kg) was

injected intraperitoneally. BiZn (0.14 mmol/kg) was administered orally by a blunt oral feeding syringe 24 hours before the cisplatin injection, just before the cisplatin injection, and then every 2 days thereafter. The mice were sacrificed by an overdose of pentobarbital. Tumor volume was calculated by the formula: $V = a^2 \cdot b \cdot \pi / 6$, where a is the short and b is the long diameter of tumor.

For assessment of *in vivo* safety/toxicity of BiZn, we treated BALB/c mice ($n = 5$) with BiZn (0.58 mmol/kg) orally for 5 days. At the time of sacrifice, brain, heart, kidney lung, and liver were collected, fixed in 10% formalin overnight, paraffin-embedded, sectioned, stained with hematoxylin and eosin, and evaluated for histology change. For assessment of the effect of BiZn on renal histology in cisplatin nephrotoxicity, we treated SCID Beige mice with 21-day high dose of cisplatin administration (day1 7.5 mg/kg, day 2 7.5/kg, and day 15 15 kg/kg) and BiZn (0.14 mmol/kg). At the time of sacrifice, kidneys were collected for histology evaluation.

For pharmacokinetic study of BALB/c mice, BiZn (0.14 mmol/kg once) was administered orally. Blood samples for determination of plasma bismuth concentrations were collected prior to and 1, 2, 4, and 6 hours after the administration. Plasma bismuth concentration was determined by inductively coupled plasma mass spectrometry (ICP-MS) as described by Hongzhe Sun et al. [29].

Bioluminescence Imaging

Bioluminescence imaging was performed on all of the mice once a week after tumor implantation. One hundred fifty micrograms per gram of D-luciferin in PBS was injected into each mouse intraperitoneally. A luminescent IVIS imaging system, equipped

with Living Imaging software (Xenogen, Alameda, CA), was used to monitor the growth of tumors in real time.

Blood Urea Nitrogen (BUN) Assay and Creatinine Assay

At the end of the study, blood collected from the mice was assessed for BUN and creatinine level. The BUN was measured using Urea Nitrogen Kit (Stanbio Laboratory, USA). The creatinine was measured using Creatinine Assay Kit (Sigma-Aldrich Co).

Statistical Analysis

The mean and SEM were computed for each treatment group. Statistically significant differences between treatment groups were detected by the one-way ANOVA test with Turkey's multiple comparison test for all pairwise multiple comparisons (Glantz SA. Primer of biostatistics, 3rd Edition., New York: McGraw Hill; 1992). Comparisons of two groups were assessed using paired Student *t* test. A *P* value of less than .05 was considered statistically significant. Three different symbols were denoted as **P* < .05, ***P* < .01, and ****P* < .001.

Results

BiZn Reduced Cisplatin-Induced Cytotoxicity In Vitro

Live cells metabolically reduce XTT to a soluble product, XTT-formazan, which can be estimated spectrophotometrically as a measure of cell viability [30]. A panel of nonmalignant cells including MSC, MIHA, C17.2, and HK-2 cells was tested. By quantifying cell

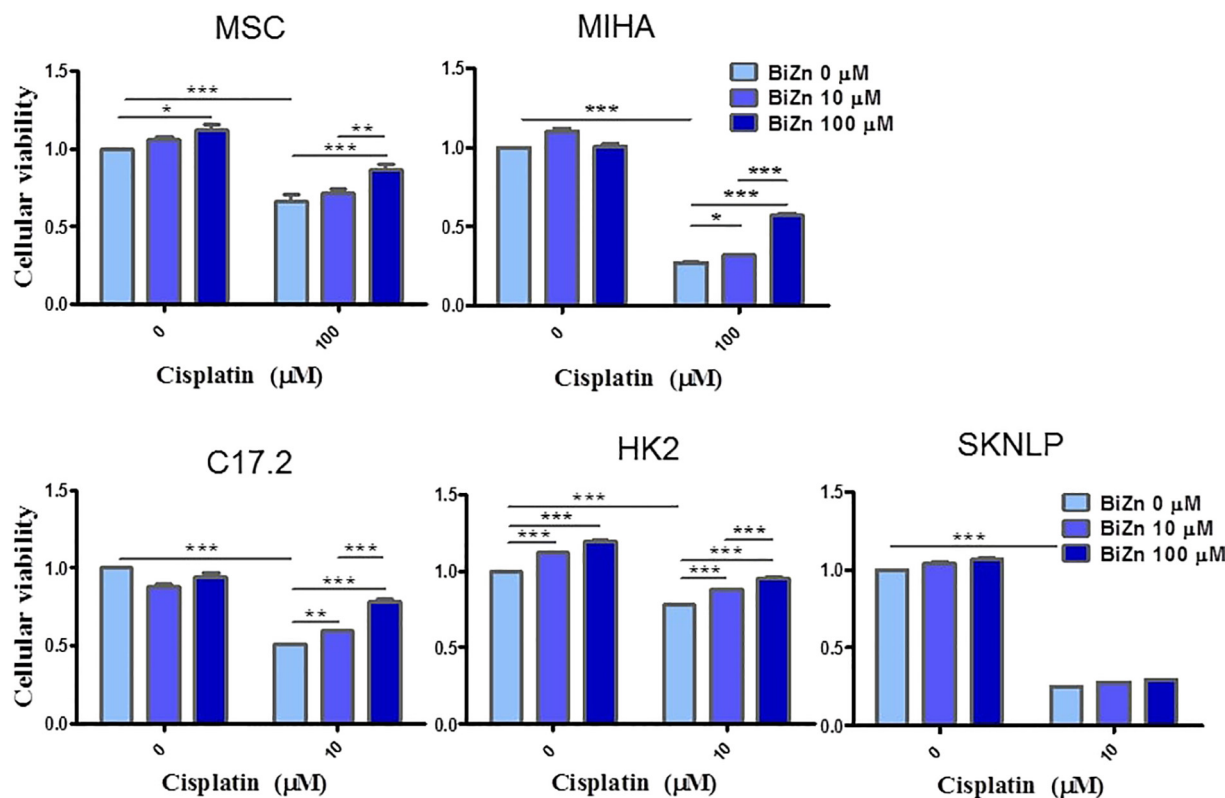


Figure 2. The cytotoxic effects of BiZn on cisplatin-treated panels of cells were analyzed by XTT assay. The protection effect of BiZn on cisplatin-treated MSC, MIHA, C17.2, HK-2, and SKNLP cell was shown. Pretreatment with BiZn significantly rescued nonmalignant cells from cisplatin-induced cytotoxicity (bismuth compounds vs. control group, ***P* < .01 and ****P* < .001).

viability, we found that BiZn did not have a toxic effect on all of the different cells when they were treated with BiZn (10 μ M or 100 μ M) alone for 2 or 3 days (Figure 2). Cisplatin induced significant cytotoxicity on C17.2, HK-2, and SKNLP cells at the concentration of 10 μ M and on MSC and MIHA cells at the concentration of 100 μ M. Furthermore, we showed that co-treatment of BiZn with cisplatin (10 μ M or 100 μ M) for 2 or 3 days could significantly rescue normal cells from cisplatin-induced cytotoxicity in a dose-dependent manner ($*P < .05$, $**P < .01$, and $***P < .001$) (Figure 2). However, for the neuroblastoma cells (SKNLP), co-treatment of BiZn with cisplatin did not show any significant protection effect (Figure 2).

Cisplatin Increased ROS Generation in HK-2 Cells But It Was Decreased by Pretreatment with BiZn. To further explore whether cisplatin can induce ROS generation and whether our new compound BiZn has potential to decrease cisplatin-induced ROS generation in HK-2 cells, DCF assay was performed on the cells loaded with cisplatin at concentration of 10 μ M and 100 μ M with pretreatment of BiZn at a concentration of 10 μ M. From our data, cisplatin induced ROS generation in HK-2 cells in a dose-dependent manner (Figure 3A). The increase in ROS generation was significantly reduced by pretreatment with BiZn (Figure 3B).

BiZn Induced the Upregulation of MT in HK-2 Cells In Vitro

One possible mechanism that accounts for the protective effect of BiZn on cisplatin-treated cells is through the induction of MT expression. To test this, protein lysates were collected and analyzed by Western blotting after treatment with BiZn. As shown in Figure 4A-a, incubation of HK-2 cells with BiZn (100 μ M) led to MT being increased significantly, suggesting that BiZn could induce MT generation from HK-2 cells. Moreover, gene expression of MT-IA and MT-IIA was significantly upregulated in HK-2 cells when compared with control cells after treatment with BiZn for 6 hours (Figure 4A-b).

MT-IIA Was Responsible for Cisplatin-Induced Cytotoxicity on HK-2 Cells

To investigate the MT-IIA function on cisplatin-induced cytotoxicity on HK-2 cells, we generated a stable MT-IIA knockdown model. We showed that, after treatment with cisplatin (10 μ M) for 48 and 72 hours, the cytotoxicity effect on MT-IIA knockdown HK-2 cells was significantly higher than the control cells ($*P < .05$) (Figure 4B), which suggested an involvement of MT-IIA on the protection effect of BiZn on cisplatin-treated cells.

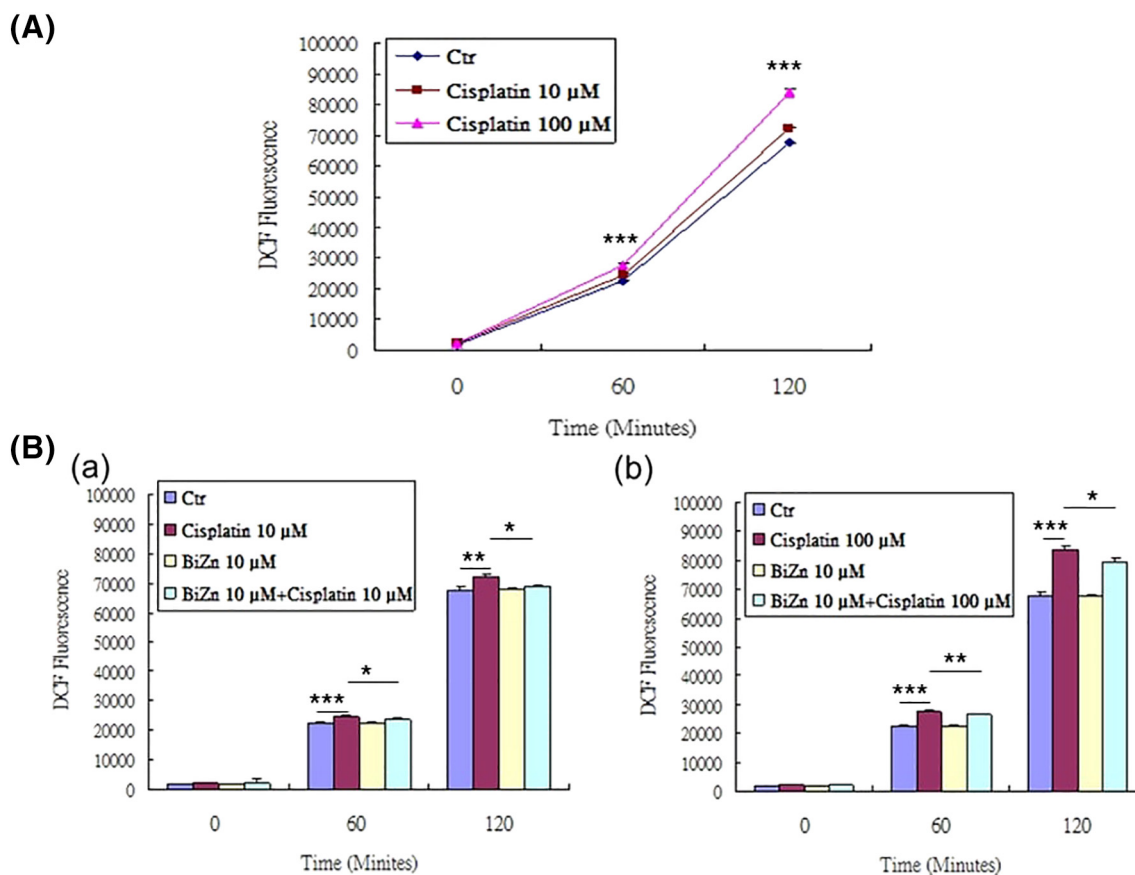


Figure 3. (A) Effect of cisplatin on HK-2 cells in inducing ROS generation. HK-2 cells were treated with cisplatin (10 μ M and 100 μ M) for 4 hours. After H₂DCF-DA staining, the amount of fluorescence produced by cisplatin-treated cells was significantly increased at 60 and 120 minutes ($n = 3$, cisplatin vs. control group, $***P < .001$). (B) Effect of BiZn on cisplatin-induced ROS generation in HK-2 cells. (B-a) Pretreatment with BiZn significantly reduced the fluorescence of H₂DCF-DA-stained low concentration (10 μ M) of cisplatin-treated cells at 60 and 120 minutes ($n = 3$, cisplatin vs. BiZn+cisplatin group, $*P < .05$). (B-b) Pretreatment with BiZn significantly reduced the fluorescence of H₂DCF-DA-stained high concentration (100 μ M) of cisplatin-treated cells at 60 and 120 minutes ($n = 3$, cisplatin vs. BiZn+cisplatin group, $**P < .01$ and $*P < .05$).

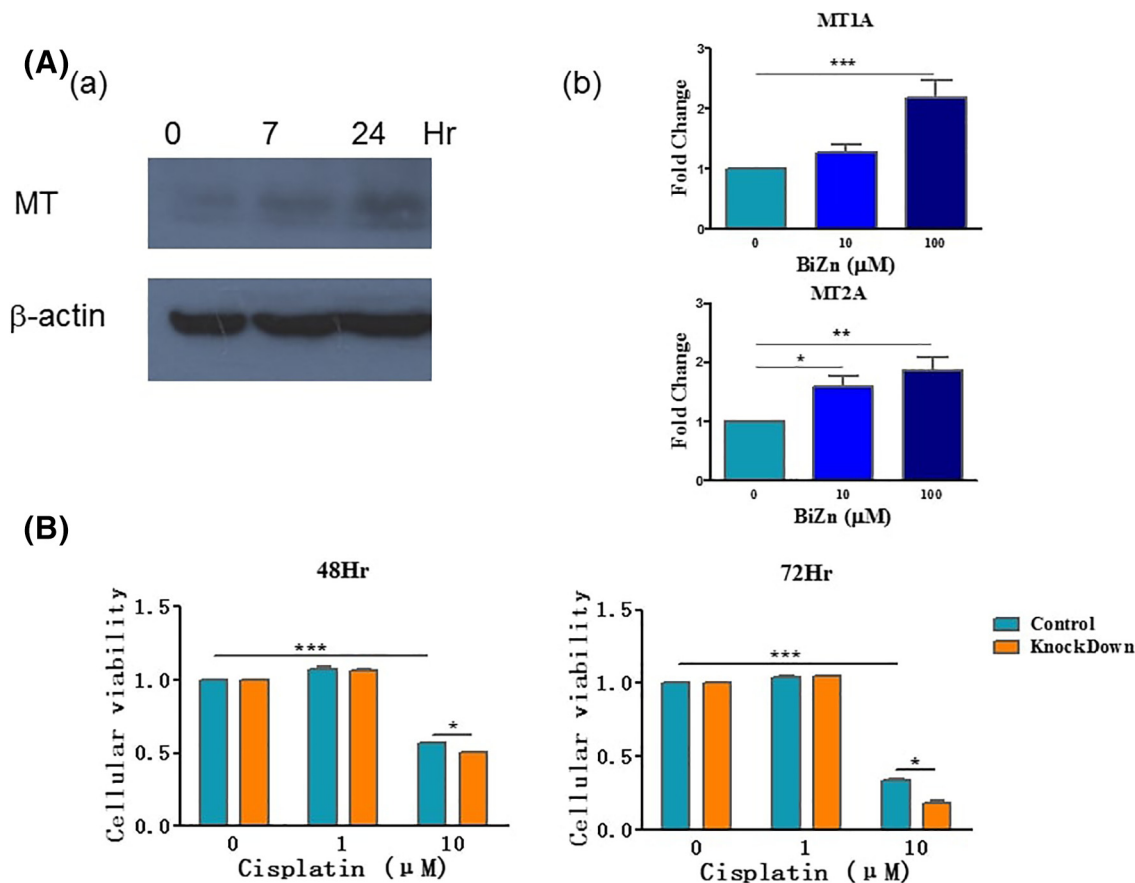


Figure 4. (A) Effect of BiZn on HK-2 cells in inducing MT protein generation. Cells were treated with BiZn (100 μ M) for the indicated time. Protein lysates were assayed by Western blotting, and beta-actin was used as the loading control. Results were representative of three independent experiments. (B) Effect of BiZn on HK-2 cells in inducing MT gene expression. Cells were treated with BiZn (10 μ M and 100 μ M) for 6 hours. MT mRNA expression was assayed by RT-qPCR. MT IA and IIA mRNA was upregulated when compared with control cells ($n = 3$, bismuth compounds vs. control group, $*P < .05$, $**P < .01$, and $***P < .001$). (C) The cytotoxic effects of cisplatin-treated HK-2 and the MT-IIA shRNA-mediated knockdown cells were analyzed by XTT assay. The effects of cisplatin-treated cells in 48 hours and 72 hours were shown. ($n = 3$, cisplatin vs. control group, $***P < .001$ and MT-IIA shRNA-mediated knockdown HK-2 cell vs. control group, $*P < .05$).

Generation of Intracellular Reduced GSH by Incubation of HK-2 Cells with BiZn

Monochlorobimane assay was used to quantify the amount of GSH generated by HK-2 cells. This probe reacts specifically with reduced GSH through GSH transferase to form a fluorescent derivative [28]. HK-2 cells stained with monochlorobimane at 37°C yielded a steady fluorescent signal. A significant increase of intracellular reduced GSH was observed upon incubation of HK-2 cells with BiZn (100 μ M) for 24 and 48 hours (Figure 5A). BSO is a potent inhibitor of GSH synthesis; incubation of HK-2 cells with 250 μ M and 500 μ M BSO for 24 and 48 hours successfully decreased the intracellular reduced GSH level (Figure 5B). These results suggest that BiZn induced GSH generation.

Reduced GSH in samples was also measured by using GSH Detection Assay Kit. A significant increase of intracellular reduced GSH was observed upon incubation of HK-2 cells with BiZn (10 and 100 μ M) for 48 hours (Figure 5C).

GSH Was Responsible for Cisplatin-Induced Cytotoxicity on HK-2 Cells

The potential role of GSH on cisplatin-induced cytotoxicity on HK-2 cells was evaluated using XTT assay and neutral red uptake

assay. Neutral red assay is one of the common methods used to detect cell viability or drug cytotoxicity. The principle of this assay is based on the detection of viable cells via the uptake of the dye neutral red. Viable cells can take up neutral red via active transport and incorporate the dye into their lysosomes, but nonviable cells cannot take up this chromophore. We found that BSO (500 μ M) was relatively nontoxic on HK-2 cells as shown in Figure 5D-a and b. BSO had a synergistic effect and enhanced the cytotoxic effect of cisplatin (10 μ M) on HK-2 cells after 48-hour incubation. This suggested that GSH was responsible for the cisplatin-induced cytotoxicity on HK-2 cells. In addition, pretreatment of HK-2 cells with BiZn followed by treatment with cisplatin+BSO for 48 hours resulted in the increased cell viability of HK-2 cells when compared with the cisplatin+BSO group (Figure 5D-a and b). The generation of intracellular reduced GSH by pretreatment of BiZn in HK-2 cells could contribute to the protection effect.

BiZn Did Not Affect the Cisplatin Antitumor Effect

The antitumor activity of cisplatin was evaluated in regular intervals for 21 days after cisplatin treatment by live imaging of mice that were orthotopically inoculated with neuroblastoma cells at the adrenal area. As shown in Figure 6A and B, treatment with BiZn did

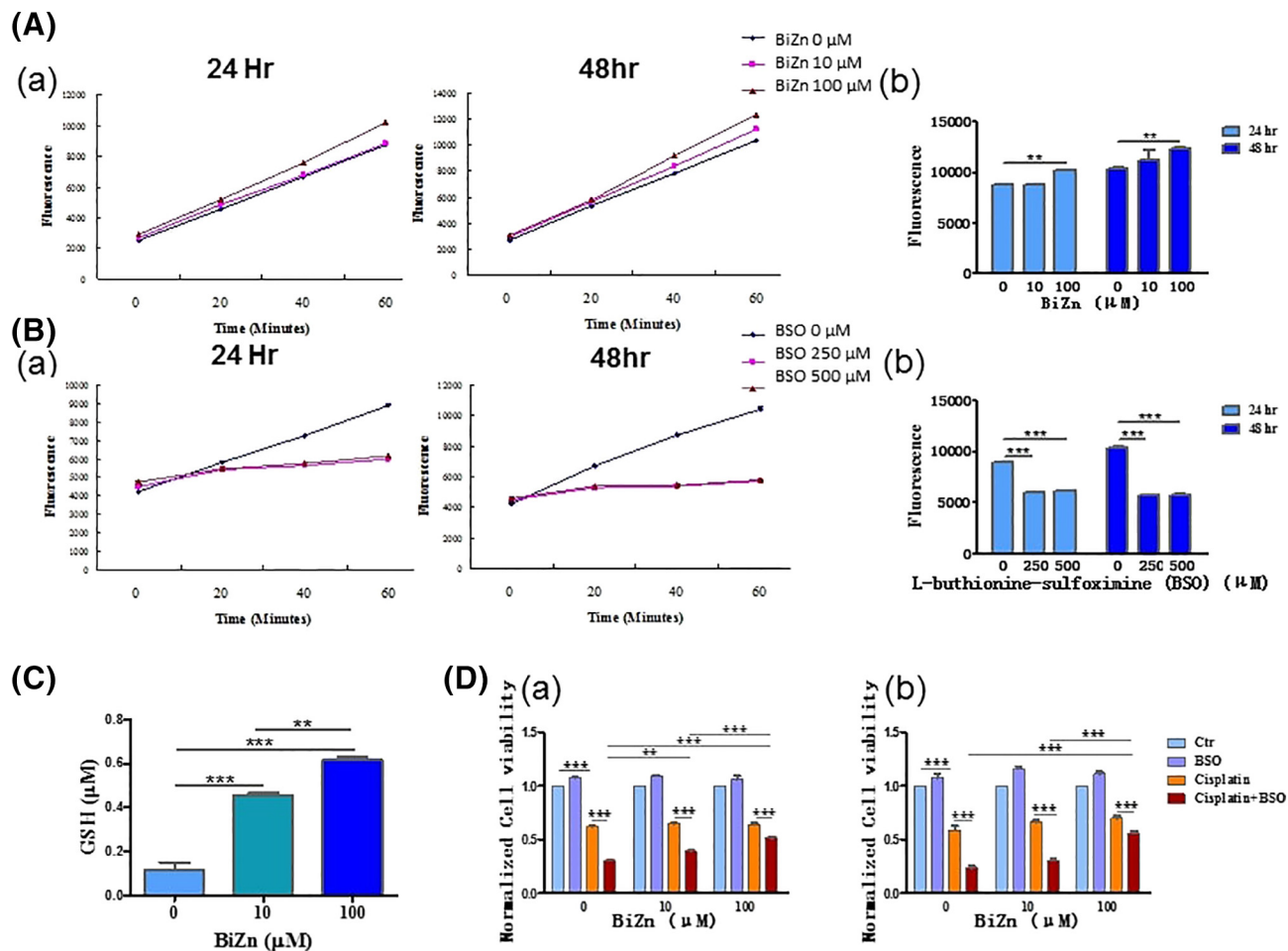


Figure 5. (A and C) Intracellular reduced GSH evaluation after 24- and 48-hour treatment with BiZn or BSO on HK-2 cells. HK-2 cells were treated with BiZn (10 μM and 100 μM) or BSO (250 μM and 500 μM) for 24 or 48 hours. After monochlorobimane staining, the fluorescence produced by the cells was measured. (A) The fluorescence increased significantly in BiZn (100 μM)-treated HK-2 cells after 24 hours of incubation ($n = 3$, BiZn 100 μM vs. control group, 60 minutes $**P < .01$) and 48 hours of incubation ($n = 3$, BiZn 100 μM vs. control group, 60 minutes $**P < .01$). (B) Monitoring the GSH depletion effect of BSO on HK-2 cells for 24 hours of incubation ($n = 3$, BSO 250 and 500 μM vs. control group, 60 minutes $***P < .001$) and 48 hours ($n = 3$, BSO 250 and 500 μM vs. control group, 60 minutes $***P < .001$) of incubation. (C) The reduced GSH increased significantly in BiZn (10 μM and 100 μM)-treated HK-2 cells after 48 hours of incubation ($n = 3$, BiZn 10 μM and 100 μM vs. control group, $***P < .001$). (D) The effects of BiZn and BSO on cisplatin-treated HK-2 cells were analyzed by XTT and neutral red uptake assay. HK-2 cells were pretreated with BiZn (10 μM and 100 μM) for 3 days before exposure to BSO (500 μM) and cisplatin (10 μM) for 48 hours. (C-a) Cell viability of HK-2 cells (XTT assay). (C-b) Cell viability of HK-2 cells (neutral red uptake assay) (compounds vs. control group or compounds vs. compounds group, $**P < .01$ and $***P < .001$).

not affect the antitumor activity of cisplatin (7.5 mg/kg, once per week for 3 weeks). Interestingly, the BiZn-treated mice had less extensive metastasis than that of control group in liver as shown in Figure 7A. Whether such findings genuinely reflected the antimetastatic effect of BiZn remains to be verified. But one thing that is very convincing was that BiZn did not affect the antitumor effect of cisplatin *in vivo* (Figure 7A and B).

BiZn Pharmacokinetics

The average concentration-time curve was shown in Figure 8A. Bismuth peak levels in serum of $24.72 \pm 1.81 \mu\text{g/l}$ were measured 1 hour after administration in mice treated with BiZn. The concentration was well below the toxic range of bismuth [28]. It was followed by rapid terminal elimination ($t_{1/2(\text{elimination})} = 1.9 \pm 0.28$ hours). Area under curve (AUC_{last}) was calculated to be $51.34 \pm 3.40 \mu\text{g h/l}$.

BiZn Did Not Have Any Toxic Effect In Vivo

Short-term treatment of mice with a high dose of BiZn (0.58 mmol/kg, every day) for 5 days showed no toxic effect on different organs (Figure 8B). Further, long-term treatment with BiZn alone (0.14 mmol/kg, every 2 days) for 3 weeks showed no toxic effect on kidneys (Figure 8D-a).

BiZn Could Reduce Cisplatin-Induced Nephrotoxicity

Histological examination revealed vacuolation, protein cast, and desquamation of epithelial cells in renal tubular epithelium 21 days after injection in the cisplatin-treated mouse as shown in Figure 8C-a. In contrast, Figure 8C-b shows the proximal renal tubules of BiZn-treated mice in which lesions appeared to be less extensive than those observed in mice that were treated with cisplatin alone. Thus, the results demonstrate a protective effect of pretreatment with BiZn against cisplatin-induced renal toxicity in SCID Beige mice.

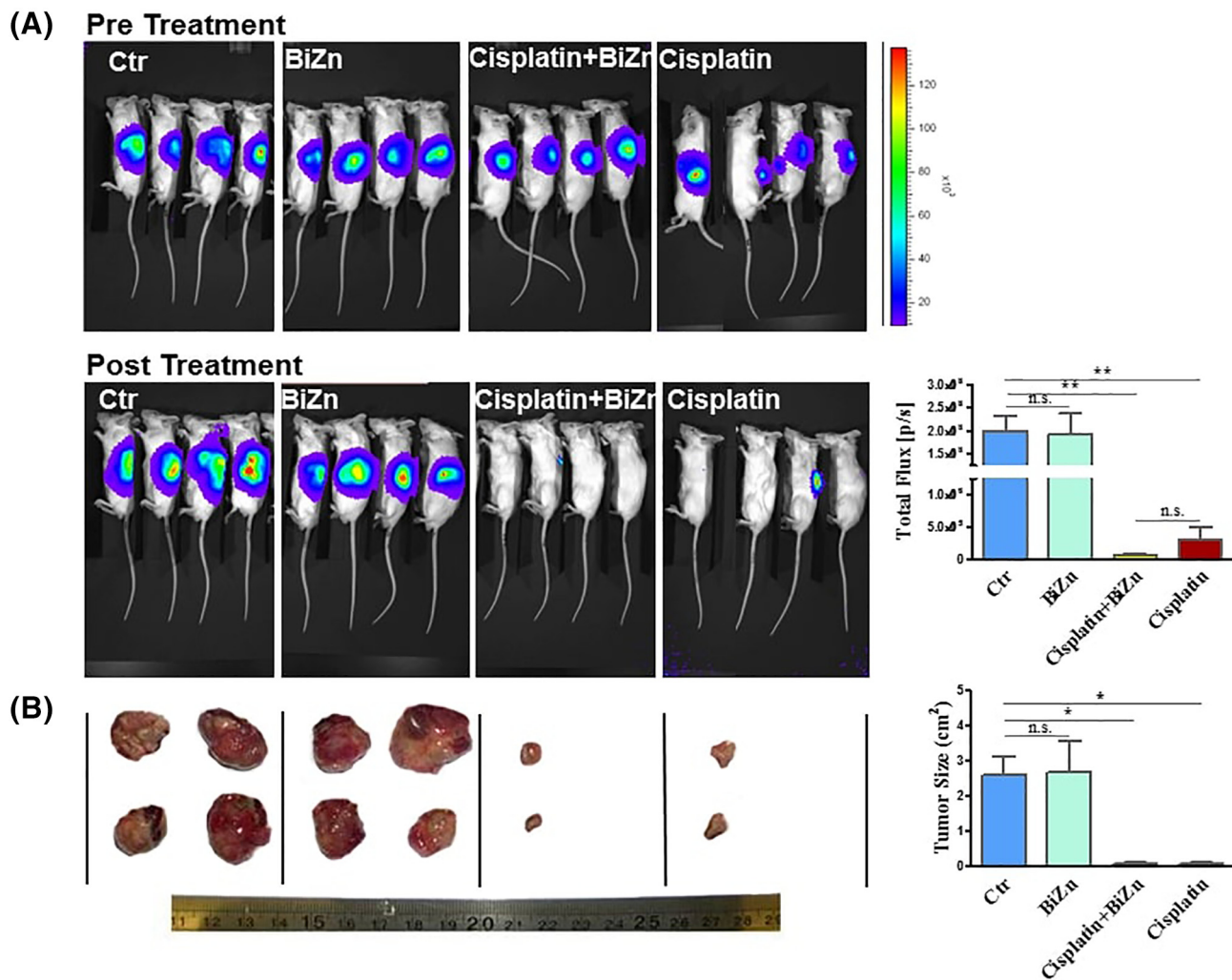


Figure 6. Administration of BiZn did not affect the antitumor effect of cisplatin on adrenal tumors. In (A), 0.2×10^6 SKNLP neuroblastoma cells were injected into mouse adrenal gland for 4 weeks to induce adrenal tumors. Mice with adrenal tumors were divided into four groups: control, BiZn-treated, cisplatin-treated, and BiZn combined with cisplatin-treated groups. Live cell imaging luciferin scan was used to evaluate the antitumor activity weekly. Three-week cisplatin- and cisplatin plus BiZn-treated tumors had significantly lower total flux when compared to control tumors (cisplatin-treated and BiZn combined with cisplatin-treated vs. control group, $**P < .01$). Cisplatin- and cisplatin plus BiZn-treated tumors had no significant difference of total flux. In (B), photos of the tumor after treatment were shown. There is a significant inhibition of tumor growth after 3 weeks cisplatin and cisplatin plus BiZn treatment (cisplatin-treated and BiZn combined with cisplatin-treated vs. control group, $*P < .05$), and there is no significant difference in tumor volume of cisplatin-treated vs. BiZn combined with cisplatin-treated group.

Cisplatin (15 mg/kg) treatment alone significantly increased BUN and creatinine levels 5 days after administration (Figure 8D-b and E). On the contrary, the addition of oral BiZn in cisplatin-treated mice significantly reduced blood BUN and creatinine levels compared with the cisplatin-treated group ($**P < .1$ and $*P < .05$) (Figure 8D-b and E). These results support the renal protective effect of BiZn on cisplatin-treated mice.

BiZn Could Improve the Survival Rate of High-Dose Cisplatin-Treated Mice

To test the toxic effect of cisplatin, the lethal dose of cisplatin was adopted. All of the mice died 12 days after treatment with high-dose cisplatin (15 mg/kg, two times) alone (Figure 8F). Co-treatment of high-dose cisplatin with BiZn (at the dose of 0.14 mmol/kg every 2 days) significantly improved the survival rate of mice under such lethal dose of cisplatin (Figure 8F). The results were demonstrated by the Kaplan-Meier analysis ($P = .001$).

Discussion

Cisplatin is a platinum-based heavy metal drug which has dual characteristics of an alkylating agent and an oxygen free radical inducer. It is currently one of the most commonly used chemotherapeutic agents for solid tumors. The main adverse side effects of cisplatin are its aural, neural, and renal toxicities. In order to attenuate these adverse side effects, we generated a new compound, BiZn (Figure 1). We demonstrated that pretreatment of BiZn decreased the cisplatin-induced renal toxicity through induction of antioxidant protein MT and antioxidant small peptide GSH.

Free radical species are a double-edged sword in the physiology of the human body. Excessive amounts disrupt many basic molecules including lipids, DNA, and proteins, resulting in severe oxidative damage within cells and leading to tissue damage [31]. Cisplatin is a ROS inducer which can inhibit cancer cell growth. Although accumulated papers demonstrate that treatment of bismuth decreases cisplatin-induced renal toxicity, whether the co-treatment of bismuth

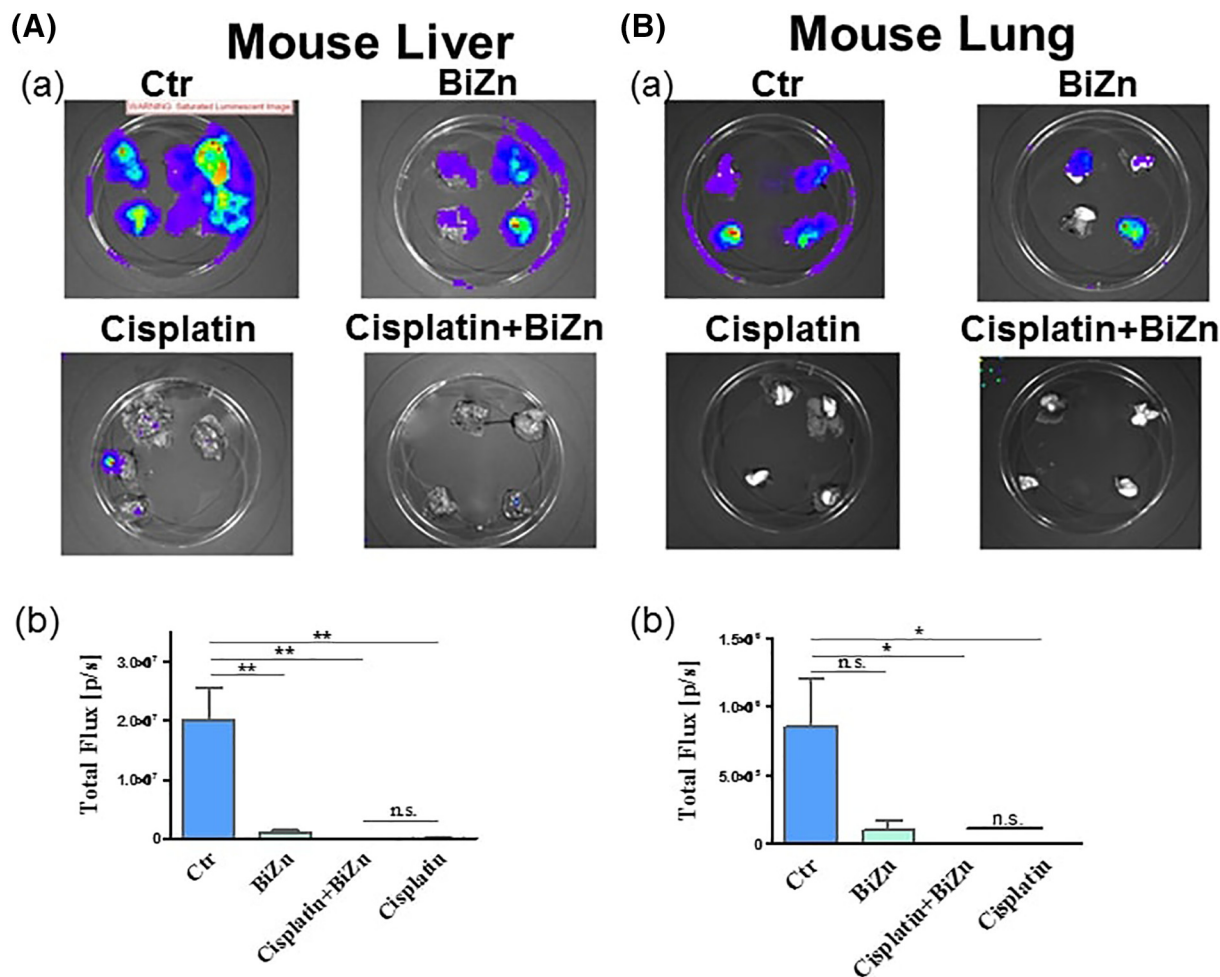


Figure 7. Administration of BiZn delayed SKNLP tumor cells lung and liver metastases. A total of 0.2×10^6 SKNLP cells were injected into the adrenal gland, and lung and liver metastases were noted. After 4-week injection of SKNLP cells, mice were treated weekly with i.p. doses of 7.5 mg/kg cisplatin for 3 weeks in cisplatin and cisplatin plus BiZn groups. For the control and BiZn-treated groups (negative control), mice were only treated for 2 weeks because of the large and rapidly progressing tumor size. Luminescence images of lungs and livers were noted. For liver groups, cisplatin- and cisplatin plus BiZn-treated livers had significantly lower total flux when compared to the control group (cisplatin-treated and BiZn combined with cisplatin-treated vs. control group, $**P < .01$). BiZn-treated livers had significantly lower total flux when compared to the control group (BiZn-treated vs. control group, $**P < .01$). Cisplatin- and cisplatin plus BiZn-treated livers had no significant difference in total flux. For lung groups, cisplatin- and cisplatin plus BiZn-treated groups had significantly lower total flux when compared to the control group (cisplatin-treated and BiZn combined with cisplatin-treated vs. control group, $*P < .05$). Cisplatin- and cisplatin plus BiZn-treated tumors had no significant difference in total flux.

inhibits cisplatin-induced ROS generation in kidney cells was still unclear. Thus, we generated our own ROS kidney cell model to investigate it. From our data, pretreatment with BiZn could inhibit cisplatin-induced ROS generation in HK-2 cells (Figure 3). Several mechanisms of bismuth protection on cisplatin-induced kidney damage have been proposed, for example, bismuth induced MT expression [32]. Previous *in vitro* studies showed that MT can serve as thiol donors to remove reactive oxygen species [33,34]. However, the mechanism related to MT-IIA on kidney cell protection by bismuth is not clear. Thus, we used shRNA to inhibit MT-IIA protein synthesis to evaluate whether MT-IIA was important for the inhibition of cisplatin-induced cell damage. Our data indicated that the cytotoxicity effect of cisplatin on MT-IIA knockdown HK-2 cells was higher than the control cells. Iron is known to induce overproduction of superoxide ($O_2^{\bullet-}$) and hydroxyl ($OH^{\bullet-}$) radicals via Fenton and Haber-Weis reaction [31,35,36]. Our previous papers showed that iron overload can induce ROS generation, which has toxic effects on

cardiovascular system, and chelator L1 could inhibit this as well as cell apoptosis [37–39]. This is in line with another publication which shows that MT could chelate iron to convert it into a form that is not active as a Fenton reactant, and the formation of an Fe-MT complex *in vitro* has been described [40,41]. Glutathione is mainly present in cells in its reduced form, GSH, which basically acts as an intracellular reductant. GSH has been shown to have antioxidant effect in preventing free radicals and heavy metal-induced cell damage [17]. Several groups have demonstrated that cisplatin induces oxidative stress in renal epithelial cells by depleting intracellular concentrations of GSH [42,43]. Our data showed that BiZn increased GSH level in kidney cells. GSH as an antioxidant may counteract the effect of ROS generated by cisplatin. Thus, the co-treatment of BiZn effectively inhibits cisplatin-induced apoptosis of kidney cells.

Bismuth (Bi) and zinc (Zn) were less toxic when compared with cadmium (Cd) and mercury (Hg); both Bi and Zn can induce higher amounts of MT in the proximal tubular cells of the kidney [44]. In

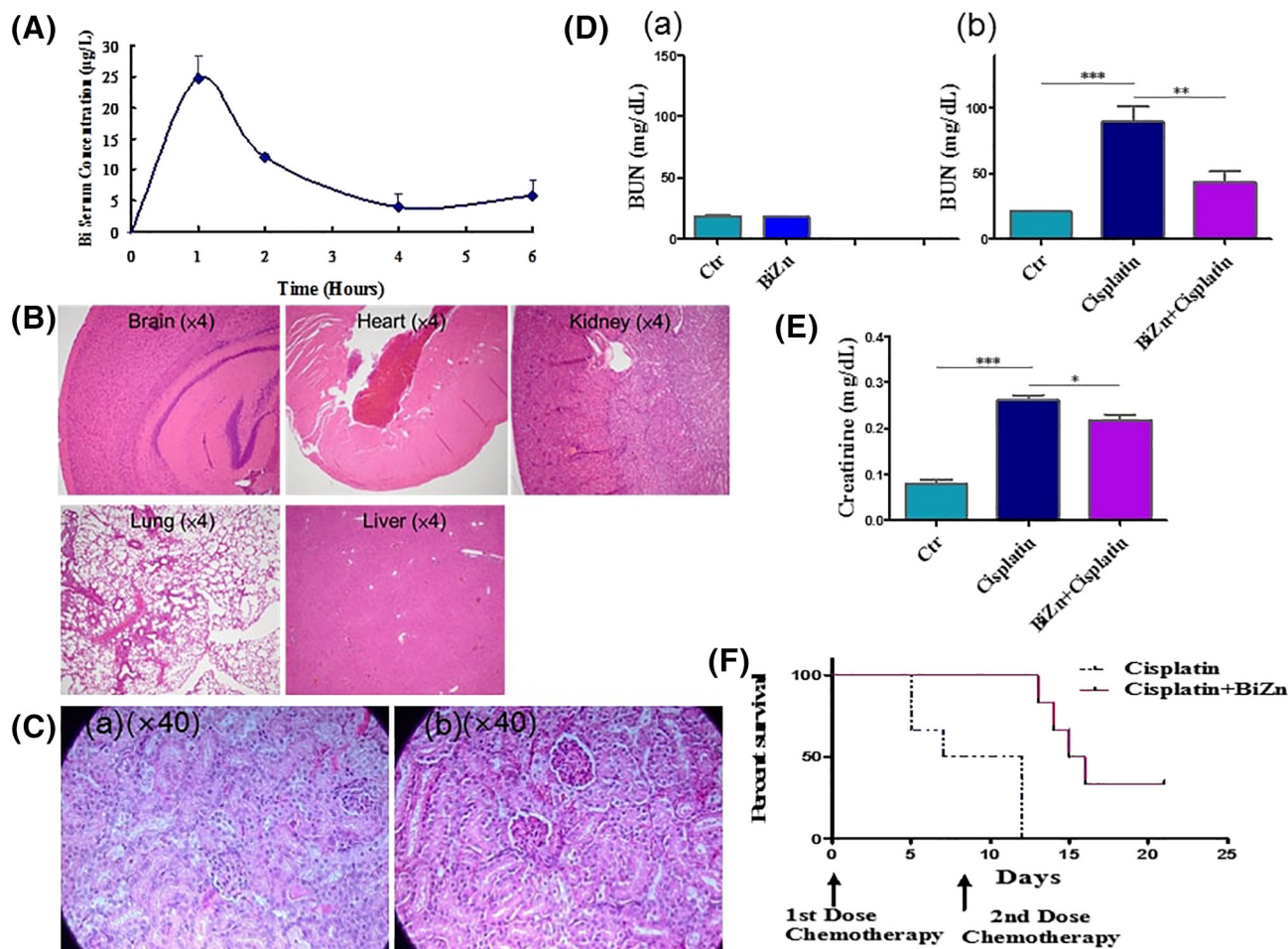


Figure 8. (A) Bismuth serum concentrations in five groups of mice with BiZn dose of 0.14 mmol/kg. The plots show the levels of bismuth content in serum as means \pm SEM over the full 6-hour time course. (B) Effect of high dose of BiZn treatment on organ histology change of mice. Mice received BiZn (0.58 mmol/kg) treatment for 5 days. Brains, hearts, kidneys, lungs, and livers were formalin-fixed, paraffin-embedded, and H&E-stained. Based on the figures, none of the organs appeared to show any evidence of brain, heart, kidney, lung, or liver damage. (C) Effect of BiZn on renal histology in cisplatin-treated SCID Beige mice. (C-a) Renal histological changes after 21 days of cisplatin administration (day 1: 7.5 mg/kg, day 2: 7.5/kg, and day 15: 15 kg/kg). (C-b) Renal histological changes with same condition of cisplatin combined with BiZn every 2 days. Photo showed protein cast, vacuolation, and desquamation of epithelial cells in the renal tubules after cisplatin administration. The injuries were attenuated by treatment of BiZn every 2-day injection. (D and E) Effect of pretreatment with BiZn on renal protection with or without cisplatin treatment on SCID Beige mice. In (D-a), mice were treated with BiZn for 3 weeks without cisplatin treatment. In (D-b and E), mice were pretreated orally with BiZn for 24 hours and just prior to cisplatin (15 mg/kg) injection. The mice were sacrificed on day 5. Blood BUN and creatinine levels were determined after the end point. Each value for BUN and creatinine represents the mean \pm SEM (BUN, $n = 6$, cisplatin vs. control group, $***P < .001$; $n = 6$ cisplatin vs. BiZn+cisplatin group, $**P < .01$) (creatinine, $n = 4$, cisplatin vs. control group, $***P < .001$; $n = 4$ cisplatin vs. BiZn+cisplatin group, $*P < .05$). (F) Survival curve of cisplatin-treated SCID Beige mice with or without treatment of BiZn. Kaplan-Meier survival curve showed that the survival of mice of cisplatin group was significantly shorter than that of mice treated with BiZn+cisplatin (log-rank statistics: cisplatin vs. BiZn+cisplatin, $***P = .001$).

this experiment, we generated a new synthetic compound, BiZn, and one advantage of using this compound is that it has low toxicity (Figure 8B and C-a) but with high MT induction ability. As Zn is an essential element in our body and Bi compounds such as colloidal bismuth subcitrate have already been used clinically in treating patients with *Helicobacter pylori* infection [45], our new combined product of BiZn is therefore potentially nontoxic. Unlike its related arsenic compound (As) in the periodic table, bismuth compound does not exert any direct cytotoxic effect on both normal and cancer cells even in high concentrations. Previous use of bismuth compounds in treating gastric mucosal-associated lymphoid tissue lymphoma was mainly based on its antibacterial function [46]. BiZn is water soluble

and can be readily absorbed by the body, which means it can be taken orally. This is an important feature because most previously available bismuth compounds were poorly absorbed and therefore have limited systemic effect upon oral administration.

We investigated the effect of this novel compound BiZn in inducing MT and GSH from kidney cells *in vitro*. We found that BiZn could induce both MT and GSH production from the HK-2 cells. Since both MT and GSH are known protective biomolecules that can protect cells from heavy metal-induced injuries, such enhancing effects of MT and GSH generation from renal cells imply a local protective effect against cisplatin-induced toxicity in the kidney. On the contrary, cisplatin has direct cytotoxic effects on all normal

cells including renal cells, hepatic cells, bone marrow–derived mesenchymal stromal cells, and neural stem cells under *in vitro* settings. Again, such cytotoxic effects could be significantly decreased by the addition of BiZn into the culture system (Figure 2). These may be based on MT and GSH induction in cells by the co-incubation with BiZn. More importantly, the protective effect of BiZn will not affect the *in vivo* cytotoxicities of cisplatin in our neuroblastoma orthotopic model.

Using our *in vivo* orthotopic model [47,48], we monitored the growth of neuroblastoma in both the local and metastatic sites. The BiZn did not affect the efficacy of cisplatin chemotherapy in both primary (adrenal) and metastatic sites such as lung and liver (Figures 6 and 7). This shows that the increased secretion of MT and GSH in kidney did not hinder the cytotoxic action of cisplatin even in these metastatic sites. In our *in vivo* model, the dosage of cisplatin that could effectively shrink the tumor does not exert high enough organ toxicity. Therefore, we were not able to clearly show the renal protection in this cohort. However, we applied lethal dose of cisplatin on another cohort of mice with and without the BiZn. Our results showed that BiZn could reduce the elevated levels of BUN caused by cisplatin treatment (Figure 8C-b). More strikingly, the oral administration of BiZn could significantly improve the survival rate under such lethal dose of cisplatin (Figure 8D). This suggested that with the help of BiZn, either higher doses of cisplatin can be used in patients with refractory tumors or organ toxicity can be minimized for those who are responsive to the conventional dosages of cisplatin.

In conclusion, we show that BiZn could effectively decrease the renal toxicity and improve the survival rate of mice treated with high-dose cisplatin, and at the same time, it did not affect the cisplatin's antitumor activity. The generation of antioxidant protein MT and antioxidant peptide GSH may partly contribute to the protection role of BiZn on cisplatin-induced kidney damage. We will further delineate the effect of BiZn on brain and liver cancer models under cisplatin therapy.

Conflict of interest in author form and attached ICMJE forms.

Acknowledgement

Innovation Technology Grant by Innovation Technology Commission of HKSAR (ITS/085/14).

References

- Attia SM (2010). The impact of quercetin on cisplatin-induced clastogenesis and apoptosis in murine marrow cells. *Mutagenesis* **25**(3), 281–288.
- Daugaard G (1990). Cisplatin nephrotoxicity: experimental and clinical studies. *Dan Med Bull* **37**(1), 1–12.
- Schweitzer VG (1993). Cisplatin-induced ototoxicity: the effect of pigmentation and inhibitory agents. *Laryngoscope* **103**(4 Pt 2), 1–52.
- Verweij J, de Wit R, and de Mulder PH (1996). Optimal control of acute cisplatin-induced emesis. *Oncology* **53**(Suppl 1), 56–64.
- Shibuya K, Cherian MG, and Satoh M (1997). Sensitivity to radiation treatment and changes in metallothionein synthesis in a transplanted murine tumor. *Radiat Res* **148**(3), 235–239.
- Ries F and Klastersky J (1986). Nephrotoxicity induced by cancer chemotherapy with special emphasis on cisplatin toxicity. *Am J Kidney Dis* **8**(5), 368–379.
- Santos NA, Bezerra CS, Martins NM, Curti C, Bianchi ML, and Santos AC (2008). Hydroxyl radical scavenger ameliorates cisplatin-induced nephrotoxicity by preventing oxidative stress, redox state unbalance, impairment of energetic metabolism and apoptosis in rat kidney mitochondria. *Cancer Chemother Pharmacol* **61**(1), 145–155.
- Block KI and Gyllenhaal C (2005). Commentary: the pharmacological antioxidant amifostine – implications of recent research for integrative cancer care. *Integr Cancer Ther* **4**(4), 329–351.
- Koukourakis MI (2003). Amifostine: is there evidence of tumor protection? *Semin Oncol* **30**(6 Suppl 18), 18–30.
- Sun H, Li H, Harvey I, and Sadler PJ (1999). Interactions of bismuth complexes with metallothionein(II). *J Biol Chem* **274**(41), 29094–29101.
- Jozefczak M, Remans T, Vangronsveld J, and Cuypers A (2012). Glutathione is a key player in metal-induced oxidative stress defenses. *Int J Mol Sci* **13**(3), 3145–3175.
- Romero-Isart N and Vasak M (2002). Advances in the structure and chemistry of metallothioneins. *J Inorg Biochem* **88**(3-4), 388–396.
- Klaassen CD, Liu J, and Diwan BA (2009). Metallothionein protection of cadmium toxicity. *Toxicol Appl Pharmacol* **238**(3), 215–220.
- Ngu TT and Stillman MJ (2009). Metalation of metallothioneins. *IUBMB Life* **61**(4), 438–446.
- Sato M and Kondoh M (2002). Recent studies on metallothionein: protection against toxicity of heavy metals and oxygen free radicals. *Toboku J Exp Med* **196**(1), 9–22.
- Futakawa N, Kondoh M, Ueda S, Higashimoto M, Takiguchi M, and Suzuki S, et al (2006). Involvement of oxidative stress in the synthesis of metallothionein induced by mitochondrial inhibitors. *Biol Pharm Bull* **29**(10), 2016–2020.
- Pompella A, Visvikis A, Paolicchi A, De Tata V, and Casini AF (2003). The changing faces of glutathione, a cellular protagonist. *Biochem Pharmacol* **66**(8), 1499–1503.
- Smyth JF, Bowman A, Perren T, Wilkinson P, Prescott RJ, and Quinn KJ, et al (1997). Glutathione reduces the toxicity and improves quality of life of women diagnosed with ovarian cancer treated with cisplatin: results of a double-blind, randomised trial. *Ann Oncol* **8**(6), 569–573.
- Li H and Sun H (2012). Recent advances in bioinorganic chemistry of bismuth. *Curr Opin Chem Biol* **16**(1-2), 74–83.
- Wang Y, Hu L, Xu F, Quan Q, Lai YT, and Xia W, et al (2017). Integrative approach for the analysis of the proteome-wide response to bismuth drugs in *Helicobacter pylori*. *Chem Sci* **8**(6), 4626–4633.
- Wang Y, Tsang CN, Xu F, Kong PW, Hu L, and Wang J, et al (2015). Bio-coordination of bismuth in *Helicobacter pylori* revealed by immobilized metal affinity chromatography. *Chem Commun (Camb)* **51**(92), 16479–16482.
- Sun H, Zhang L, and Szeto KY (2004). Bismuth in medicine. *Met Ions Biol Syst* **41**, 333–378.
- Chang YY, Lai YT, Cheng T, Wang H, Yang Y, and Sun H (2015). Selective interaction of Hpn-like protein with nickel, zinc and bismuth in vitro and in cells by FRET. *J Inorg Biochem* **142**, 8–14.
- Wang R, Lai TP, Gao P, Zhang H, Ho PL, and Woo PC, et al (2018). Bismuth antimicrobial drugs serve as broad-spectrum metallo-beta-lactamase inhibitors. *Nat Commun* **9**(1), 439.
- Kagi JH and Schaffer A (1988). Biochemistry of metallothionein. *Biochemistry* **27**(23), 8509–8515.
- Kobayashi K, Shida R, Hasegawa T, Satoh M, Seko Y, and Tohyama C, et al (2005). Induction of hepatic metallothionein by trivalent cerium: role of interleukin 6. *Biol Pharm Bull* **28**(10), 1859–1863.
- Borenfreund E and Puerner JA (1984). A simple quantitative procedure using monolayer cultures for cytotoxicity assays. *J Tissue Cult Methods* **9**, 7–9.
- Yue TL, Ma XL, Wang X, Romanic AM, Liu GL, and Loudon C, et al (1998). Possible involvement of stress-activated protein kinase signaling pathway and Fas receptor expression in prevention of ischemia/reperfusion-induced cardiomyocyte apoptosis by carvedilol. *Circ Res* **82**(2), 166–174.
- Sun H and Szeto KY (2003). Binding of bismuth to serum proteins: implication for targets of Bi(III) in blood plasma. *J Inorg Biochem* **94**(1-2), 114–120.
- Weislow OS, Kiser R, Fine DL, Bader J, Shoemaker RH, and Boyd MR (1989). New soluble-formazan assay for HIV-1 cytopathic effects: application to high-flux screening of synthetic and natural products for AIDS-antiviral activity. *J Natl Cancer Inst* **81**(8), 577–586.
- Valko M, Morris H, and Cronin MT (2005). Metals, toxicity and oxidative stress. *Curr Med Chem* **12**(10), 1161–1208.
- Boogaard PJ, Slikkerveer A, Nagelkerke JF, and Mulder GJ (1991). The role of metallothionein in the reduction of cisplatin-induced nephrotoxicity by Bi3(+)-pretreatment in the rat in vivo and in vitro. Are antioxidant properties of metallothionein more relevant than platinum binding. *Biochem Pharmacol* **41**(3), 369–375.
- Hamer DH (1986). Metallothionein. *Annu Rev Biochem* **55**, 913–951.

- [34] Lazo JS, Kondo Y, Dellapiazza D, Michalska AE, Choo KH, and Pitt BR (1995). Enhanced sensitivity to oxidative stress in cultured embryonic cells from transgenic mice deficient in metallothionein I and II genes. *J Biol Chem* **270**(10), 5506–5510.
- [35] Braughler JM, Duncan LA, and Chase RL (1986). The involvement of iron in lipid peroxidation. Importance of ferric to ferrous ratios in initiation. *J Biol Chem* **261**(22), 10282–10289.
- [36] Halliwell B (2007). Biochemistry of oxidative stress. *Biochem Soc Trans* **35**(Pt 5), 1147–1150.
- [37] Chan S, Chen MP, Cao JM, Chan GC, and Cheung YF (2014). Carvedilol protects against iron-induced microparticle generation and apoptosis of endothelial cells. *Acta Haematol* **132**(2), 200–210.
- [38] Chan S, Chan GC, Ye J, Lian Q, Chen J, and Yang M (2015). Thrombopoietin Protects Cardiomyocytes from Iron-Overload Induced Oxidative Stress and Mitochondrial Injury. *Cell Physiol Biochem* **36**(5), 2063–2071.
- [39] Chan S, Lian Q, Chen MP, Jiang D, Ho JTK, and Cheung YF, et al (2018). Deferiprone inhibits iron overload-induced tissue factor bearing endothelial microparticle generation by inhibition oxidative stress induced mitochondrial injury, and apoptosis. *Toxicol Appl Pharmacol* **338**, 148–158. <https://doi.org/10.1016/j.taap.2017.11.005>.
- [40] Good M and Vasak M (1986). Iron(II)-substituted metallothionein: evidence for the existence of iron-thiolate clusters. *Biochemistry* **25**(26), 8353–8356.
- [41] Mello-Filho AC, Chubatsu LS, and Meneghini R (1988). V79 Chinese-hamster cells rendered resistant to high cadmium concentration also become resistant to oxidative stress. *Biochem J* **256**(2), 475–479.
- [42] Husain K, Morris C, Whitworth C, Trammell GL, Rybak LP, and Somani SM (1998). Protection by ebselen against cisplatin-induced nephrotoxicity: antioxidant system. *Mol Cell Biochem* **178**(1-2), 127–133.
- [43] Huang Q, Dunn II RT, Jayadev S, DiSorbo O, Pack FD, and Farr SB, et al (2001). Assessment of cisplatin-induced nephrotoxicity by microarray technology. *Toxicol Sci* **63**(2), 196–207.
- [44] Moffatt P and Denizau F (1997). Metallothionein in physiological and pathophysiological processes. *Drug Metab Rev* **29**(1-2), 261–307.
- [45] Whitehead MW, Phillips RH, Sieniawska CE, Delves HT, Seed PT, and Thompson RP, et al (2000). Double-blind comparison of absorbable colloidal bismuth subcitrate and nonabsorbable bismuth subnitrate in the eradication of *Helicobacter pylori* and the relief of nonulcer dyspepsia. *Helicobacter* **5**(3), 169–175.
- [46] Guo Q, Guo S, and Zhang Y (2013). Treatment of gastric MALT lymphoma with a focus on *Helicobacter pylori* eradication. *Int J Hematol* **97**(6), 735–742.
- [47] Guo ZL, Yu B, Ning BT, Chan S, Lin QB, and Li JC, et al (2015). Genetically modified "obligate" anaerobic *Salmonella typhimurium* as a therapeutic strategy for neuroblastoma. *J Hematol Oncol* **8**, 99.
- [48] Guo ZL, Richardson DR, Kalinowski DS, Kovacevic Z, Tan-Un KC, and Chan GC (2016). The novel thiosemicarbazone, di-2-pyridylketone 4-cyclohexyl-4-methyl-3-thiosemicarbazone (DpC), inhibits neuroblastoma growth in vitro and in vivo via multiple mechanisms. *J Hematol Oncol* **9**(1), 98.